ELSEVIER

Contents lists available at ScienceDirect

Polyhedron

journal homepage: www.elsevier.com/locate/poly



New $Mn^{II}Mn_8^{III}$ and $Mn_2^{II}Mn_{10}^{III}Mn_2^{IV}$ clusters from the reaction of methyl 2-pyridyl ketone oxime with $[Mn_{12}O_{12}(O_2CR)_{16}(H_2O)_4]$



Tuhin Ghosh, Khalil A. Abboud, George Christou*

Department of Chemistry, University of Florida, Gainesville, FL 32611-7200, USA

ARTICLE INFO

Article history: Received 28 August 2019 Accepted 6 September 2019 Available online 11 September 2019

Dedicated to the founding in 2019 of the Molecular Magnetism in North America (MAGNA) workshop.

Keywords: Manganese Cluster Crystal structure Magnetism

ABSTRACT

The syntheses, crystal structures and magnetic properties of two mixed-valence Mn clusters $[Mn^{II}Mn_8^{II}O_6(mpko)_3(O_2CMe)_{11}]$ (1) and $[Mn_2^{II}Mn_1^{II}Mn_2^{IV}O_{12}(mpko)_6(O_2CPh)_{12}(H_2O)_2]$ (2) are reported. They were obtained from the corresponding reactions in MeCN of $[Mn_{12}O_{12}(O_2CR)_{16}(H_2O)_4]$ (R = Me (3), Ph (4)) with eight equivalents of methyl(pyridine-2-yl)ketone oxime (mpkoH). The cores of 1 and 2 are structurally related: 1 possesses a $[Mn_9(\mu_3-O)_6]^{14+}$ core with an unusual topology comprising a near-planar Mn^{III} -centered Mn_6^{II} hexagon with additional Mn^{II} and Mn^{III} ions above and below the plane. Complex 2 possesses a $[Mn_{14}(\mu_4-O)_2(\mu_3-O)_{10}]^{18+}$ core that can be described as a dimer of two Mn_7 incomplete-cores of 1. It is also a rare example of a Mn cluster containing three Mn oxidation states. Fits of variable-temperature, solid-state dc magnetic susceptibility data collected in a 0.1 T field in the 5.0–300 K range established that 1 and 2 possess ground state spins of $S = ^3/_2$ and S = 1, respectively, which were confirmed by ac in-phase susceptibility data.

© 2019 Elsevier Ltd. All rights reserved.

1. Introduction

The synthesis and characterization of new polynuclear coordination clusters of paramagnetic metal ions continue to be an active area of research. Such studies are stimulated by a wide range of diverse reasons, including relevance to biology, medicine, catalysis, and many others. For example, our own interest in Mn/O clusters over many years has primarily resulted from its importance in bioinorganic chemistry [1-5] and molecular magnetism [6], the former from the occurrence of Mn in various enzymatic systems such as the {Mn₄Ca} unit of the photosynthetic oxygen evolving complex (OEC) of plants and cyanobacteria [7], and the latter from the fascinating magnetic properties that Mn/O clusters often exhibit, including single-molecule magnetism. The latter are individual molecules that behave as single-domain nanoscale magnetic particles at low temperature [8-12] and also exhibit fascinating quantum phenomena such as quantum tunneling of magnetization [13,14], quantum phase interference [15–18] and quantum superposition/entanglement [19–21]. The $[Mn_{12}O_{12}(O_2CR)_{16}(H_2O)_4]$ family (Mn_{12}) of clusters has been known since 1980 [22] and is one of the best and most thoroughly studied SMMs to date [12,23,24]. Mn₁₂ clusters are also excellent starting materials for subsequent chemistry, including changes to the cluster's carboxylate ligands [25,26], its oxidation state [27], or the structure/nuclearity. The latter usually occurs in reactions with chelates [28] or destabilization by reduction [29] or alcoholysis [30].

In a parallel direction, we have been interested in the use of methyl(2-pyridyl)ketone oxime (mpkoH) in Mn chemistry, owing to its ability to act as both a chelate and a bridging ligand, o⁻ has led to the formation of numerous polynuclear compounds [31–36]. In addition, mpko⁻ ligand has a propensity to promote ferromagnetic interactions in Mn clusters [37], which has also been the

mpkoH

basis of our work in supramolecular oligomers of Mn_3 SMMs with S = 6 formed from dioximate and dicarboxylate linkers [38–40]. Since we had never explored the reactions of mpkoH with Mn_{12} clusters, we have investigated such reactions in the present work, anticipating a significant change to the Mn_{12} nuclearity and/or structure. We herein report the results of this study, the

^{*} Corresponding author.

E-mail address: christou@chem.ufl.edu (G. Christou).

syntheses, crystal structures and magnetochemical characterization of two new high nuclearity manganese complexes, $[Mn_9(\mu_3-O)_6(mpko)_3(O_2CCH_3)_{11}]$ (1) and $[Mn_{14}(\mu_4-O)_2(\mu_3-O)_4-(mpko)_6(O_2CPh)_{12}]$ (2).

2. Experimental section

2.1. Syntheses

All preparations were performed under aerobic conditions using chemicals and solvents as received, unless otherwise stated. $[Mn_{12}O_{12}(O_2CMe)_{16}(H_2O)_4]\cdot 2MeCO_2H\cdot 4H_2O$ (3) was prepared as described elsewhere [22]. $[Mn_{12}O_{12}(O_2CPh)_{16}(H_2O)_4]$ (4) was prepared from 3 by the carboxylate substitution procedure described elsewhere involving removal under reduced pressure of an acetic acid/toluene azeotrope [12,41]. mpkoH was synthesized as described [42].

2.1.1. $[Mn^{II}Mn_8^{III}O_6(mpko)_3(O_2CMe)_{11}]$ (1)

To a stirred, dark brown solution of **3** (0.21 g, 0.10 mmol) in MeCN (25 mL) was added mpkoH (0.11 g, 0.80 mmol). The solution was stirred for one hour, filtered, and the filtrate allowed to stand for slow evaporation at ambient temperature. Dark brown X-ray quality crystals of **1**-4MeCN slowly grew over 3 days. They were collected by filtration, washed with Et₂O (2 × 5 mL), and dried under vacuum; the yield was $\sim\!\!46\%$ based on Mn. Anal. Calc. (Found) for **1**-H₂O (C₄₃H₅₆Mn₉N₆O₃₂): C 31.05 (31.33); H 3.39 (3.61); N 5.05 (4.84)%. Selected IR data (KBr, cm $^{-1}$): 3418(br), 1556(s), 1417(s), 1345(w), 1155(m), 1105(m), 1079(m), 1048(w), 777(w), 713(m), 616(s), 418(w).

2.1.2. $[Mn_2^{II}Mn_{10}^{II}Mn_2^{IV}O_{12}(mpko)_6(O_2CPh)_{12}(H_2O)_2]$ (2)

Method A. To a stirred, dark brown solution of **4** (0.28 g, 0.10 mmol) in MeCN (25 mL) was added mpkoH (0.11 g, 0.80 mmol). The solution was stirred for one hour, filtered, and the dark-brown filtrate allowed to stand for slow evaporation at ambient temperature. Dark brown X-ray quality crystals of **2**-xMeCN-yH₂O slowly grew over 5 days. They were collected by filtration, washed with Et₂O (2 \times 5 mL), and dried under vacuum; the yield was \sim 60% based on Mn. *Anal.* Calc. (Found) for **2**-H₂O (C₁₂₆-H₁₀₈Mn₁₄N₁₂O₄₅): C 46.15 (46.22); H 3.32 (3.39); N 5.13 (5.02)%. Selected IR data (KBr, cm⁻¹): 3431(br), 3063(w), 1599(s), 1559(s), 1447(w), 1405(s), 1175(m), 1151(m), 1068(s), 1025(m), 841(w), 777(w), 716(s), 675(s), 607(s), 459(w), 429(w).

Method B. To a stirred, dark brown solution of **4** (0.28 g, 0.10 mmol) in MeCN (25 mL) was added mpkoH (0.11 g, 0.80 g). The solution was stirred for one hour and the solvent then removed under partial vacuum by rotary evaporation. The residue was dissolved in CH₂Cl₂ (25 mL), filtered, and the filtrate allowed to stand undisturbed in a sealed vial at ambient temperature. Dark brown X-ray quality crystals slowly grew over 3 days. They were collected by filtration, washed with Et₂O (2 × 5 mL), and dried under vacuum; the yield was ~45% based on Mn. The IR spectrum and magnetic data confirmed the product to be the same as from Method A.

Method C. To a stirred, dark brown solution of **4** (0.28 g, 0.10 mmol) in CH_2Cl_2 (25 mL) was added mpkoH (0.11 g, 0.80 g). The solution was stirred for an hour, filtered, and the filtrate allowed to stand undisturbed in a sealed vial at ambient temperature. Dark brown X-ray quality crystals slowly grew over 3 days. They were collected by filtration, washed with Et_2O (2 \times 5 mL), and dried under vacuum; the yield was \sim 40% based on Mn. The IR spectrum and magnetic data confirmed the product to be the same as from Method A.

2.2. General and physical measurements

Infrared spectra were recorded in the solid state (KBr pellets) on a Nicolet Nexus 670 FTIR spectrometer in the 400–4000 cm⁻¹ range. Elemental analyses were performed by Atlantic Microlab, Inc. Variable-temperature direct current (dc) and alternating current (ac) magnetic susceptibility data were collected using a Quantum Design MPMS-XL SQUID magnetometer equipped with a 7 T dc magnet and operating in the 1.8–400 K range. Samples were embedded in solid eicosane to prevent torquing. Ac magnetic susceptibility measurements were performed in a 3.5 G ac field and zero dc field at oscillation frequencies in the 50–1000 Hz range. Pascal's constants were used to estimate the diamagnetic correction, which were subtracted from the experimental susceptibilities to give the molar paramagnetic susceptibility ($\gamma_{\rm M}$) [43].

2.3. Single-crystal X-ray crystallography

Crystallographic data and structure refinement details for $1 \cdot 4 \text{MeCN}$ and $2 \cdot x \text{MeCN} \cdot y \text{H}_2 \text{O}$ are summarized in Table 1. Diffraction data were collected at 100 K on a Bruker DUO diffractometer using MoK α radiation (λ = 0.71073 Å) and an APEXII CCD area detector. Raw data frames were read by program SAINT [44] and integrated using 3D profiling algorithms. The resulting data were reduced to produce hkl reflections and their intensities and estimated standard deviations. The data were corrected for Lorentz and polarization effects and numerical absorption corrections were applied based on indexed and measured faces. The structures were solved and refined on F^2 in SHELXTL2014, using full-matrix least-squares refinement. The non-H atoms were refined with anisotropic thermal parameters, and all the H atoms except those in the lattice solvent molecules were placed in calculated idealized positions and refined as riding on their parent atoms.

For **1**-4MeCN, the asymmetric unit consists of a Mn_9 cluster and four MeCN solvent molecules; the latter refined with 0.75 occupancies. In the final cycle of refinement, 15,808 reflections (of which 7809 are observed with $I > 2\sigma(I)$) were used to refine 928

Table 1
Crystal data and structure refinement parameters for 1·4MeCN and 2·xMeCN·yH₂O.

Parameter	1	2
Formula ^a	C ₄₃ H ₅₄ Mn ₉ N ₆ O ₃₁	C ₁₂₆ H ₁₀₆ Mn ₁₄ N ₁₂ O ₄₄
$FW (g mol^{-1})^{a}$	1645.35	3261.37
Crystal size (mm)	$0.169 \times 0.100 \times 0.023$	$0.230 \times 0.108 \times 0.032$
Crystal system	monoclinic	orthorhombic
Space group	P2 ₁ /c	Pca2 ₁
a (Å)	12.2527(15)	25.853(3)
b (Å)	22.320(3)	21.165(2)
c (Å)	25.201(3)	27.508(3)
В (°)	91.179(2)	90
Z	4	4
T (K)	100(2)	100(2)
λ (Å)	0.71073	0.71073
$ ho_{ m calc}$ (g/cm $^{-3}$)	1.705	1.661
μ (mm ⁻¹)	1.682	1.223
θ range (°)	1.616-27.499	1.447-27.500
Collected reflections	74,208	233,855
Unique reflections	15,808	34,585
R _{int}	0.1273	0.1236
Reflections $I > 2\sigma(I)$)	7809	16,659
Final R ₁ ^{b,c}	0.0468	0.0559
Final wR2 ^{b,d}	0.0896	0.1406
$\Delta ho_{ m max, \ min}$ (e Å $^{-3}$)	0.904, -0.605	0.734, -0.535

^a Excluding lattice solvent molecules.

^b $I > 2\sigma(I)$).

^c $R_1 = \Sigma(||F_o| - |F_c||)/\Sigma|F_o|$.

^d $wR_2 = [\Sigma[w(F_o^2 - F_c^2)^2]/\Sigma[w(F_o^2)^2]]^{1/2}$.

Table 2Bond valence sum (BVS)^a calculations for Mn atoms in **1**.

Atom	Mn ^{II}	Mn ^{III}	Mn ^{IV}
Mn1	1.88	1.62	1.81
Mn2	3.27	3.05	3.10
Mn3	3.26	3.04	3.10
Mn4	3.20	2.92	3.32
Mn5	3.37	3.17	3.19
Mn6	3.19	2.92	3.32
Mn7	3.21	2.88	3.26
Mn8	3.15	2.88	3.26
Mn9	3.31	3.09	3.13

^a The bold value is the closest to the charge for which it was calculated. The oxidation state is the nearest whole number to this value.

parameters, and the resulting R_1 , wR_2 and S (goodness of fit) were 4.68%, 8.96% and 0.858, respectively.

For 2•xMeCN•yH₂O, the asymmetric unit consists of a Mn₁₄ cluster, approximately twelve MeCN solvent molecules and some water molecules. The solvent molecules were all disordered and could not be modeled properly, thus program SQUEEZE [45], a part of the PLATON [46] package of crystallographic software, was used to calculate the solvent disorder area and remove its contribution to the overall intensity data. The intensity contribution of the water (one half and one quarter molecules) could not be removed due to their proximity to disorder regions of the cluster, and their H atoms could not be located and were not included in the final refinement model. There are six disorder regions in the cluster: one is the pyridyl ring of one mpko group (atoms C1-C4 disordered against C1'-C4'); the second disorder is of the Ph rings in the two benzoate ligands at opposite ends of the cluster, which were refined in three positions each; and the last disorder is of three other benzoate Ph rings, which were refined in two positions each. For all disorder regions, site occupancy factors were restrained to add up to unity. In the case of triply-disordered rings, command SUMP was used in the final refinement. The Ueq of atoms of each disordered PART were restrained to be equivalent. In the final cycle of refinement, 34,585 reflections (of which 16,659 are observed with I > 2 $\sigma(I)$) were used to refine 1627 parameters, and the resulting R_1 , wR_2 and S (goodness of fit) were 5.59%, 14.06% and 0.955, respectively.

3. Results and discussion

3.1. Syntheses

The Mn/RCO $_2$ /mpkoH reaction system has been extensively studied over the last ten years or so, yielding a variety of polynuclear Mn clusters with aesthetically beautiful motifs, large ground state spin values, and SMM behavior [31–37,40,47,48]. Two representative examples are the [Mn $_3$ O(mpko) $_3$ (O $_2$ CR) $_3$] $^+$ (R = Me, Et, Ph) cations with an S=6 ground state [37], and [Mn $_9$ O $_6$ (O $_2$ CMe) $_7$ (O $_3$ -PPh) $_2$ (mpko) $_3$ (H $_2$ O)] with S=1 [47]. In one extension of our work in this area, we have recently explored the reaction of mpkoH with members of the [Mn $_1$ 2O $_1$ 2(O $_2$ CR) $_1$ 6(H $_2$ O) $_4$] family of mixed-valence (8Mn $_1$ 1, 4Mn $_1$ 1) as a possible route to new high-nuclearity clusters.

A number of Mn_{12} :mpkoH ratios and reaction solvent(s) were explored in the course of developing the following successful reactions to pure products. Thus, the reaction of $[Mn_{12}O_{12}(O_2CMe)_{16}(H_2O)_4]$ (3)) and mpkoH in a 1:8 molar ratio in MeCN gave no noticeable color change to the dark brown solution, but upon filtration and slow evaporation of the filtrate afforded dark brown crystals of the new mixed-valence complex $[Mn_9O_6(mpko)_3(O_2CMe)_{11}]$ (1; Mn^{II} , $8Mn^{III}$) in \sim 46% yield. Small changes in the Mn_{12} :mpkoH ratio gave the same product in comparable yield.

Since changes to the carboxylate can often lead to significantly different products in Mn carboxylate chemistry, we also explored the analogous reaction of $[Mn_{12}O_{12}(O_2CPh)_{16}(H_2O)_4]$ (4) and mpkoH in MeCN, and this led to dark brown crystals of a different mixed-valence product, $[Mn_{14}O_{12}(mpko)_6(O_2CPh)_{12}(H_2O)_2]$ (2; $2Mn^{II}$, $10Mn^{III}$, $2Mn^{IV}$) in \sim 60% yield (Method A of Section 2.1.2). 2 could also be obtained, but in lower isolated yields of \sim 40–45%, from a two-step procedure using MeCN and then CH_2CI_2 (Method B), or simply changing the solvent in Method A from MeCN to CH_2CI_2 (Method C).

The average Mn oxidation state in **1** and **2** are similar (+2.9 and +3.0, respectively) and both are lower than the +3.33 in **3** and **4**. The only reasonable reducing agent in the reaction is mpkoH, and it may thus be more than a coincidence that the Mn₁₂: mpkoH = 1:8 reaction ratio (i.e., Mn:mpkoH = 3:2) is also larger than those in **1** and **2**, i.e. Mn:mpko = 3:1 and 7:3, respectively. In other words, the Mn₁₂:mpkoH = 1:8 reaction ratio, found optimum to yield **1** and **2** in good yield, represents an excess of mpkoH that can provide the necessary reducing agent for product formation. Of course, Mn disproportionation might have occurred instead, but we could not isolate any other product from the filtrate after products were collected and so we cannot assess this possibility any further.

3.2. Description of structures

A stereoview of the complete structure of **1** and its labeled core are shown in Fig. 1. Selected bond distances and angles are listed in Table S1 (see Supplementary Material). Complex **1** crystallizes in the monoclinic space group $P2_1/c$ with the complete Mn_9 cluster in the asymmetric unit. The $[Mn_9(\mu_3-O^{2-})_6]^{14+}$ core contains a Mn_7 subunit consisting of a Mn_6^{II} hexagon with the seventh Mn_1^{II} (Mn_5) at its center, and attached either side of the Mn_7 unit via two of its O^{2-} ions (O1 and O6) are a Mn_1^{II} (Mn_1) on one side and a Mn_1^{III} (Mn_2) on the other to give a chair-like conformation. The

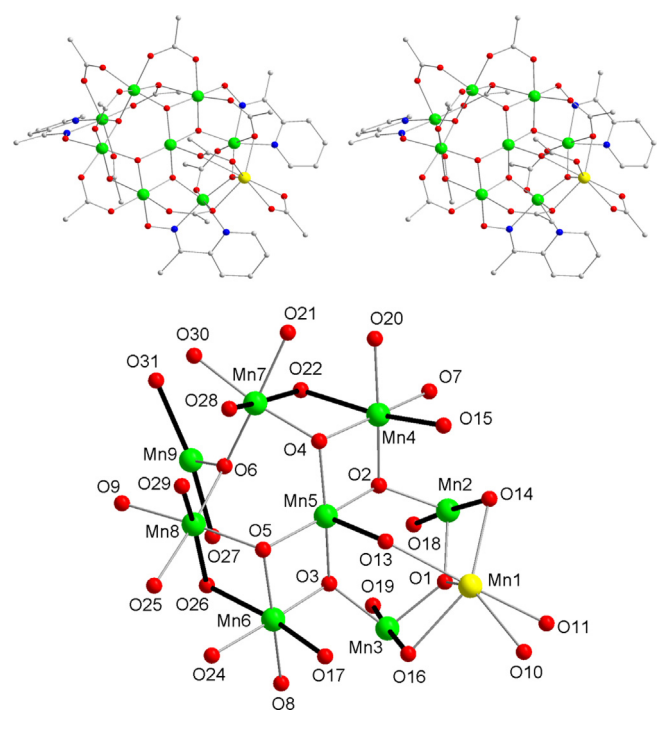


Fig. 1. Stereopair of complete complex **1**, with H atoms omitted for clarity, and its labeled core. Mn^{III} JT axes are shown as thicker bonds. Colour code: Mn^{II} yellow; Mn^{III} green; O red; N blue; C gray. (Colour online.)

Mn₆ hexagon is distorted from planarity by a slight folding about the Mn4/Mn6 'hinge' giving a dihedral angle between the Mn(4,6,7,8) and Mn(2,3,4,6) planes of 161,22°. Additional distortions result from the central Mn5 being slightly below the Mn4···Mn6 vector, giving a Mn4-Mn5-Mn6 angle of 170.61(10)°, and the significant range of Mn••Mn separations (3.069(2)–3.352(2) Å) in the hexagon as a result of the three different types of bridging ligand sets on the six Mn··Mn edges. The Mn oxidation states were determined from their metric parameters and the Jahn-Teller (JT) axial elongation expected for Mn^{III} ions in near-octahedral geometry, and confirmed by bond valence sum (BVS) calculations (Table 2) [49]. Oxygen atoms O1-O6 all had BVS values (Table S2) consistent with non-protonation, i.e. O²⁻ ions. All Mn^{III} ions are six-coordinate octahedral, except square-pyramidal Mn5 (τ = 0.01, where τ = 0 and 1 for perfect square-pyramidal and trigonal bipyramidal geometry, respectively [50]) and the Mn^{II} ion (Mn1) is seven-coordinate. Peripheral ligation in 1 is provided by three mpko- groups in their usual chelating/ bridging mode and ten acetate groups in four different binding modes (Fig. 2), including a single chelating acetate on the Mn^{II} ion.

A stereoview of the complete structure of **2** and its labeled core are shown in Fig. 3. Selected bond distances and angles are listed in Table S3 (see Supplementary Material). Complex **2** crystallizes in the orthorhombic space group Pca2₁ with the complete Mn₁₄ cluster in the asymmetric unit. The $[Mn_{14}(\mu_4-O^2)_2(\mu_3-O^2)_{10}]^{18+}$ core can be conveniently separated into three units: a central $[Mn_4^{III}-Mn_2^{IV}(\mu_3-O)_4(\mu-O)_4]^{4+}$ subunit (Mn5-Mn10) that comprises a $\{Mn_4O_6\}$ face-fused 'incomplete-dicubane' (Mn5,6,9,10) and

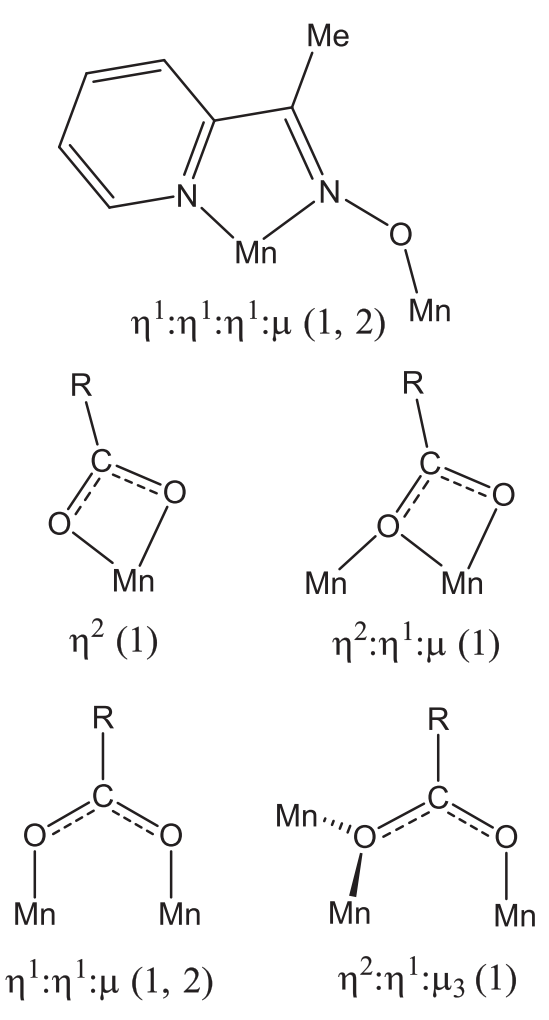


Fig. 2. Binding modes of mpko- and carboxylate groups in 1 and 2.

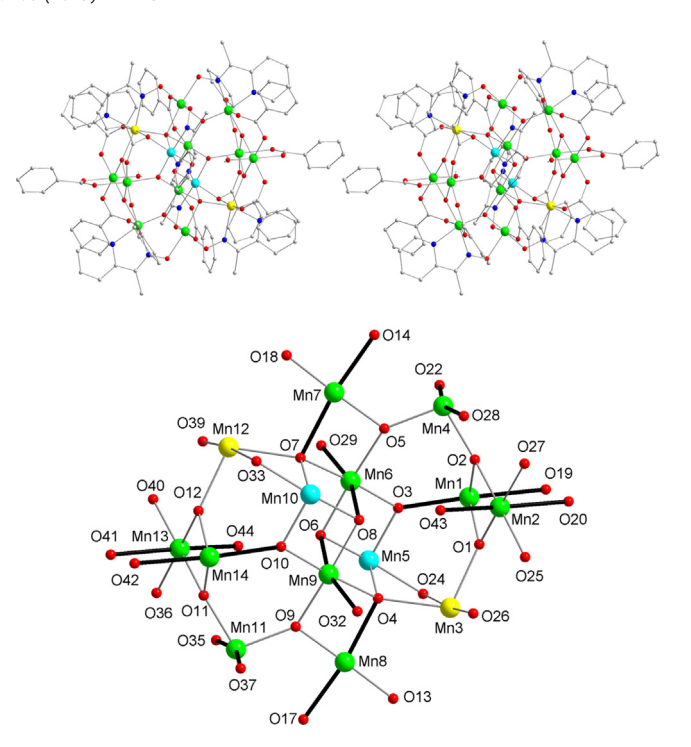


Fig. 3. Stereopair of complete complex **2**, with H atoms omitted for clarity, and its labeled core. Mn^{III} JT axes are shown as thicker bonds. Colour code: Mn^{II} yellow; Mn^{III} green; Mn^{IV} turquoise; O red; N blue; C gray. (Colour online.)

O3,4,6,7,8,10), which is a common unit in discrete form in Mn/O chemistry [51], to which is attached another Mn and O^{2-} at each end (Mn7O5 and Mn8O9). The central $\{Mn_4O_6\}$ is then attached by its O^{2-} ions on either side to two $[Mn^{II}Mn_3^{III}(\mu_3-O)_2]^{7+}$ 'butterfly' subunits, which are again common units in Mn/O chemistry, including at this mixed-valent oxidation state [52]. The Mn oxidation states were determined as for 1, and the Mn and O BVS values are listed in Tables 3 and S4. This revealed a 2Mn^{II}, 10Mn^{III} and 2Mn^{IV} description for 2, with Mn3/Mn12 and Mn5/Mn10 being the Mn^{II} and Mn^{ÎV} ions, respectively. The Mn^{II} ions are five-coordinate square pyramidal (τ = 0.03 and 0.01 for Mn3 and Mn12) but there are close contacts to both of them from benzoate O atoms (Mn3···O24 = 2.539 (8), $Mn12 \cdot \cdot \cdot O33 = 2.558(8)$ Å) so they could reasonably be described as very distorted octahedral. The Mn^{IV} ions are six-coordinate octahedral, as are all the Mn^{III} ions, which display JT axial elongations. The O BVS calculations also confirm O1-O12 to be unprotonated (i.e., O^{2-}) and O43/O44 to be doubly-protonated (i.e., H_2O ligands).

Table 3Bond valence sum (BVS)^a calculations for Mn atoms in **2**.

	(-,		
Atom	Mn ^{II}	Mn ^{III}	Mn ^{IV}
Mn1	3.32	2.95	3.10
Mn2	3.18	2.91	3.30
Mn3	1.85	1.72	1.76
Mn4	3.32	3.10	3.16
Mn5	3.90	3.63	3.71
Mn6	3.23	2.96	3.34
Mn7	3.31	3.03	3.40
Mn8	3.44	3.15	3.55
Mn9	3.24	2.97	3.36
Mn10	4.05	3.77	3.88
Mn11	3.26	3.04	3.09
Mn12	1.76	1.65	1.68
Mn13	3.15	2.88	3.26
Mn14	3.25	2.97	3.34

^a The bold value is the closest to the charge for which it was calculated. The oxidation state is the nearest whole number to this value.

Peripheral ligation in **2** is provided by six mpko $^-$ groups in the same chelating/bridging mode as in **1** (Fig. 2), twelve benzoates all in the common syn,syn $\eta^1:\eta^1:\mu$ mode, and two terminal H₂O ligands on Mn2/Mn13.

Neither **1** nor **2** exhibit any significant inter-cluster interactions, other than the many weak contacts involving C—H units typical of molecular crystals of materials with organic peripheries. The two H_2O ligands in **2** form intramolecular hydrogen-bonding contacts with benzoate O atoms (O···O = 2.561(10) and 2.615 (10) Å), and even with twelve benzoates per cluster, there are no significant intermolecular π ·· π stacking interactions.

There are a number of Mn_9 and Mn_{14} clusters already in the literature, including a few with mpko⁻ groups, and these are collected in Tables 4 and 5, respectively. Table 4 shows that 1 is the second example of a $Mn^{II}Mn_8^{II}$ cluster, the previous one, $[Mn_9O_6(O_2-CMe)_7(O_3PPh)_2(mpko)_3(H_2O)]$, also contains mpko⁻ groups but exhi-

Table 4 Formulas, oxidation states, and ground state spin S values of enneanuclear Mn/O clusters.

Complex ^{a,b}	Oxidation level	S	Ref.
[Mn ₉ O ₇ (O ₂ CMe) ₁₁ (thme)(py) ₃ (H ₂ O)]	$Mn_2^{II}Mn_4^{III}Mn_3^{IV}$	$^{17}/_{2}$	[56]
$[Mn_9O_7(O_2CMe)_{11}(tmp)(py)_3(H_2O)_2]$	$Mn_2^{II}Mn_4^{III}Mn_3^{IV}$	$^{17}/_{2}$	[57]
$[Mn_9O_4(OMe)_4(O_2CMe)_3(Me\text{-sao})_6(H_2O)]$	Mn ₉ ^{III}	6	[58]
[Mn ₉ O ₄ (OH)(OMe) ₃ (O ₂ CMe) ₃ (Me-	Mn_9^{III}	6	[59]
sao ₆ (MeOH) ₂] [Mn ₉ O ₄ (OMe) ₃ (O ₂ CMe) ₃ (naphthsao) ₆ (solv)]	Mn_{o}^{III}	6	[60]
$[Mn_9O_2(bzox)_{11(bzoxH)(MeOH)_4(H_2O)_2}]^+$	MngIII	3	[61]
[Mn9O6(O2CCH3)11(mpko)6]	Mn ^{II} Mn ₈	$^{3}/_{2}$	t.w.
[Mn9O7(O2CPh)13(dmhp)2]	Mnglii	2	[62]
$[Mn_9O_7(O_2CBu^t)_{13}(MeCN)_2]$	MngIII	1	[63]
$[Mn_9O_6(CO_3)(O_2CPe^t)_{12}(H_2O)_2]$	MngIII	0	[64]
$[Mn_9O_6(O_2CMe)_4(pao)_8(Hpao)_2]$	$Mn_4^{II}Mn_4^{III}Mn^{IV}$	n.r.	[53]
$[Mn_9O_6(O_2CMe)_7(O_3PPh)_2(mpko)_3(H_2O)]$	Mn ^{II} Mn ₈	5/2	[47]

^a Counterions omitted for clarity.

bits a very different core topology to $\mathbf{1}$ [47]. In contrast, $[Mn_9O_6(O_2CMe)_4(pao)_8(Hpao)_2]$ has a similar core structure with $\mathbf{1}$ but at a different oxidation level, $Mn_4^{II}Mn_4^{III}Mn_1^{III}Mn_2^{IV}$ oxidation state, the previous being $[Mn_{14}O_8(Hpyaox)_{14}(pyaox)_2(N_3)_2]^{6+}$ [54] but with a very different core topology. Similarly, no previous Mn_{14} complex at any oxidation state has a similar core to $\mathbf{2}$. The highest nuclearity Mn/mpko cluster is $[Mn_{16}O_8(O_2CPh)_{14}(mpko)_4(dpkd)_4]$, where $dpkd^{2-}$ is the gem-diolate form of di-2-pyridylketone [48]. We are unaware of any heterometallic Mn/mpko clusters, and the largest with any metal is $[Ln_3Ni_3(H_2O)_3(mpko)_9(O_2)(NO_3)_3]$ (ClO₄), where Ln = Gd, Dy [55].

3.3. Magnetochemistry

Variable-temperature dc and ac magnetic susceptibility data for vacuum-dried $\mathbf{1}\cdot\mathbf{H}_2\mathbf{0}$ and $\mathbf{2}\cdot\mathbf{H}_2\mathbf{0}$ in a 0.1 T field and in the 5.0 – 300 K temperature range were collected on a crushed microcrystalline sample of $\mathbf{1}$ restrained in eicosane to prevent torqueing. The obtained data are plotted as $\chi_{\rm M}T$ vs. T shown in Fig. 4.

For $1 \cdot H_2O$, the $\chi_M T$ is 27.10 cm³ K mol⁻¹ at 300 K, slightly less than the spin-only (g = 2) value for a Mn^{II}Mn₈^{III} cluster with noninteracting ions (28.38 cm³ K mol⁻¹), and it decreases steadily with decreasing temperature to 2.67 cm³ K mol⁻¹ at 5.0 K. This profile is indicative of dominant antiferromagnetic (AF) interactions between the metal centers, and the 5.0 K value suggests a small spin ground state for **1** of $S = \frac{1}{2}$ or $\frac{3}{2}$. The high nuclearity and low symmetry of the Mn₉ core, and the resulting number of inequivalent pairwise Mn··Mn exchange coupling parameters (Jii), preclude fitting of the 5.0–300 K data. We instead attempted to fit magnetization (M) data collected at dc magnetic fields and temperatures in the 1-70 kG and 1.8-10.0 K ranges, but could not get acceptable fits even when data at higher fields were excluded. This is a common problem created by the presence of a high density of low-lying excited states, especially in AF systems where these low-lying states have S values greater than the ground state. The fact that even just using low-field data doesn't solve the problem indicates particularly low-lying excited states, and this is consistent with the high Mn nuclearity and the presence of Mn^{II}, which gives weak exchange couplings.

For ${\bf 2}\cdot {\bf H}_2{\bf O}$, $\chi_M T$ steadily decreases with decreasing temperature from $40.89~{\rm cm}^3~{\rm K~mol}^{-1}$ at $300~{\rm K}$ to $25.18~{\rm cm}^3~{\rm K~mol}^{-1}$ at $45.0~{\rm K}$, and then decreases more rapidly to $4.28~{\rm cm}^3~{\rm K~mol}^{-1}$ at $5.0~{\rm K}$.

Table 5 Formulas, oxidation states, and ground state spin S values of tetradecanuclear Mn/O clusters.

Complex ^{a,b}	Oxidation states	S	Refs.
[Mn ₁₄ O ₄ (OH) ₄ (L1) ₄ (O ₂ CPh) ₁₄ (OMe) ₂]	Mn ₆ ^{II} Mn ₈ ^{III}	2	[65]
$[Mn_{14}(L2)_8(HL2)_2(H_2O)_2(MeOH)_{14}]$	$Mn_4^{II}Mn_{10}^{III}$	n.r.	[66]
$[Mn_{14}O_2(OH)_4(ppo)_{18}(Hppo)_4(NO_3)_4(MeCN)_4]$	$Mn_{12}^{II}Mn_{2}^{III}$	0	[67]
$[Mn_{14}O_4(OH)_2(OCN)_6(O_2CMe)_2(L3)_8(solv)]^{2+}$	$Mn_6^{II}Mn_8^{III}$	9	[68]
$[Mn_{14}O_4(O_2CMe)_{20}(L3)_4]$	$Mn_{10}^{II}Mn_{4}^{III}$	0	[69]
$[Mn_{14}O_2(OH)_4(OMe)_4(O_2CMe)_2(L4)_2-(HL4)_4(H_2L4)_2(solv')]^{2+}$	$Mn^{\mathrm{II}}_{2}Mn^{\mathrm{III}}_{12}$	11/2	[70]
[Mn14(OH)3Cl(BSC4A)3(tBuPO3)6(H2O)(MeOH)]	Mn_{14}^{II}	n.r.	[71]
$[Mn_{14}(OH)_2(Hpeol)_4(H_2peol)_6I_4(EtOH)_6]^{4+}$	$Mn_8^{II}Mn_6^{III}$	7 ± 1	[72]
$[Mn_{14}O_8(HL5)_{14}(L5)_2(N_3)_2]^{6+}$	$Mn_2^{II}Mn_{10}^{III}Mn_2^{IV}$	6	[54]
$[Mn_{14}O_{12}(OH)_6(HL6)_6(bpy)_6]^{4+}$	$Mn_2^{III}Mn_6^{IIV}Mn_6^{IV}$	n.r.	[73]
$[Mn_{14}O_{12}(mpko)_6(O_2CPh)_{12}(H_2O)_2]$	$Mn_2^{II}Mn_{10}^{III}Mn_2^{IV}$	1	t.w.
$[Mn_{14}O_7(OH)_2(CI)_4(^tBuPO_3H)(^tBuPO_3)_{10}(L7)]^{2-}$	$Mn_3^{II}Mn_{11}^{III}$	$\geq^{35}/_{2}$	[74]
$[Mn_{14}(CO_3)(OH)_6(HL8)_6(HL9)_3(H_2O)_3]^{4-}$	Mn ^{II}	5/2	[75]
$[Mn_{14}O_{12}(EtCO_2)_{12}(pd)_4(EtOH)_4(py)_4]^{2^+}$	$Mn_{10}^{III}Mn_{4}^{IV}$	1	[76]

^a Counterions are omitted for clarity.

 $[\]label{eq:balance} \begin{array}{llll} ^b \ Abbreviations: & n.r. = not & reported; & t.w. = this & work; & H_3thme = 1,1,1-tris(hydroxymethyl)ethane; & H_3tmp = 1,1,1-tris(hydroxymethyl)propane; \\ Me-saoH_2 = 2-hydroxyphenylethanone & oxime; & naphthsaoH_2 = 1-(1-hydroxynaph-thalen-2-yl)-ethanone & oxime; & bzoxH_2 = α-benzoin & oxime; & dmhp = 2,4-dimethyl-6-hydroxypyrimidine; & Pe^tCO_2H = 2,2-dimethylbutyric & acid; & Hpao = 2-pyridineal-doxime; & solv = (MeOH)_X(H_2O)_y. \end{array}$

b Abbreviations: n.r. = not reported; t.w. = this work; $H_2L1 = N$ -salicylidene-o-aminophenol; $H_4L2 = (Z)$ -3-(salicylhydrazinocarbonyl) propenoic acid; $H_2P_3 = P_3$ -phenyl-3-pyrazolin-5-one; $H_2L3 = P_3$ -diol form of di-2-pyridyl ketone; $H_4L4 = (2,6-bis(5-(2-hydroxyphenyl)-pyrazol-3-yl)-pyridine; <math>H_4P_3$ -petert-butylsulfonylcalix|4|arene; H_3P_3 -petert-butylphosphonic acid; H_4P_3 -petert-butylph

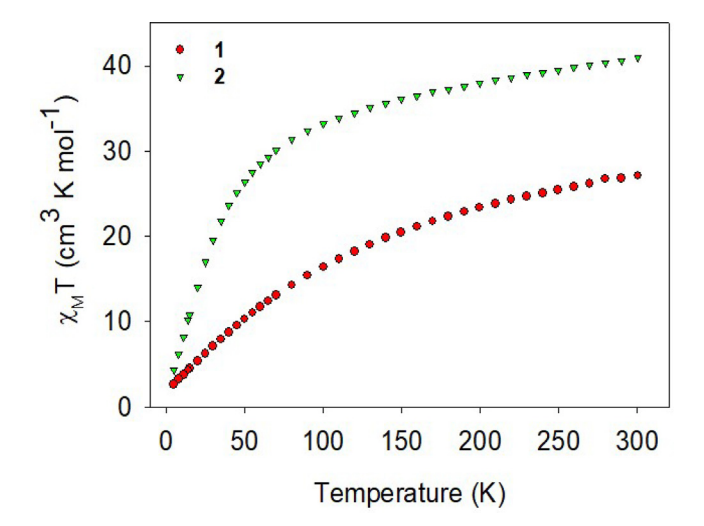


Fig. 4. $\chi_M T$ vs. T plots for complexes 1·H₂O and 2·H₂O in a 0.1 T (1000 G) applied dc

The 300 K value is again less than the spin-only 42.5 cm³ K mol⁻¹ for a Mn₂^{II}Mn₁₀^{III}Mn₂^{IV} cluster with non-interacting metal centers, and the plot profile again indicates dominant AF exchange interactions in the molecule. The 5.0 K value suggests that 2 possesses a ground state spin of S = 1 or S = 2. As for 1, the high metal nuclearity and low symmetry of **2** prevented fitting of the $\chi_M T$ vs. T data or of the *M* data collected at low fields and temperatures.

As an alternative probe of the ground state, ac magnetic susceptibility data were collected in the 1.8-15.0 K range using zero dc field and a 3.5 G ac field with oscillation frequencies in the 50-1000 Hz range. The resulting in-phase (χ'_{M}) components of the ac susceptibility signals are shown as $\chi'_{M}T$ vs. T plots in Fig. 5. For $1 \cdot H_2O$, γ'_MT decreases steadily with decreasing temperature from 4.75 cm³ K mol⁻¹ at 15 K to 2.00 cm³ K mol⁻¹ at 1.8 K, indicating depopulation of excited states with S larger than the ground state. Extrapolation of the data from above 3.0 (to avoid the effect of weak intermolecular interactions) to 0 K, where only the ground state will be populated, gives a value of $\sim 1.8 \text{ cm}^3 \text{ K mol}^{-1}$ indicating an $S = {}^3/_2$ ground state with $g \sim 1.96$. For **2**·H₂O, $\chi'_M T$ decreases steeply with decreasing temperature from 7.66 cm³ K mol⁻¹ at 15 K to 1.58 cm³ K mol⁻¹ at 1.8 K, consistent with depopulation of a high density of low-lying excited states, as expected from the high nuclearity. Extrapolation of the data to 0 K gives $\sim 1 \text{ cm}^3$ K mol⁻¹ indicating an S = 1 ground state with $g \sim 2$. As expected, neither $1 \cdot H_2O$ nor $2 \cdot H_2O$ exhibited an out-of-phase (χ''_M) ac susceptibility signal down to 1.8 K (Figs. S3 and S4).

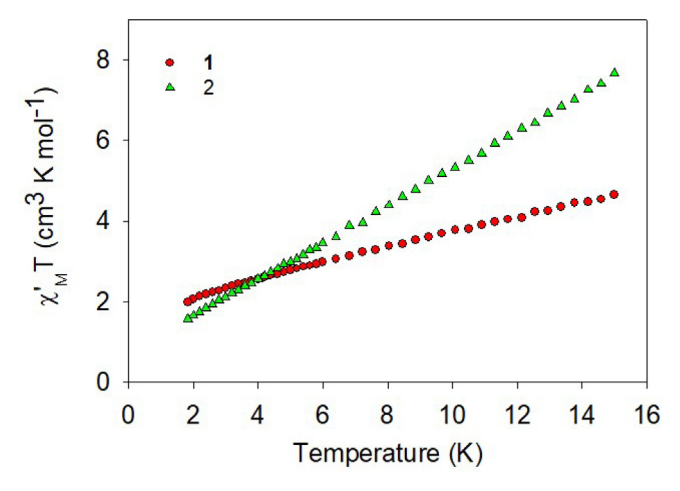


Fig. 5. AC in-phase $\chi'_{M}T$ vs. T plots for $\mathbf{1}\cdot H_{2}O$ and $\mathbf{2}\cdot H_{2}O$ in the 1.8–15.0 K range.

4. Conclusions

The use of mpkoH in Mn/O cluster chemistry in the present work has provided a further demonstration of its ability to yield complexes with interesting structures as a result of its chelating and bridging abilities, in this case giving Mn9 and Mn14 cluster products with related core subunits. Along the same lines, the [Mn₁₂O₁₂(O₂CR)₁₆(H₂O)₄] family have once again proven themselves to be convenient sources of Mn^{III}/Mn^{IV} reagents for subsequent reactions with chelates targeted at the synthesis of new cluster types.

Acknowledgment

This work was supported by the US National Science Foundation (Grant CHE-1900321).

Appendix A. Supplementary data

CCDC 1948598 and 1948599 contains the supplementary crystallographic data for 1.4MeCN and 2.xMeCN.yH2O, respectively. These data can be obtained free of charge via http://www. ccdc.cam.ac.uk/conts/retrieving.html, or from the Cambridge Crystallographic Data Centre, 12 Union Road, Cambridge CB2 1EZ, UK; fax: (+44) 1223-336-033; or e-mail: deposit@ccdc.cam.ac.uk.

Supplementary data to this article can be found online at https://doi.org/10.1016/j.poly.2019.114145.

References

- [1] V.K. Yachandra, K. Sauer, M.P. Klein, Chem. Rev. 96 (1996) 2927.
- [2] K.N. Ferreira, T.M. Iverson, K. Maghlaoui, J. Barber, S. Iwata, Science 303 (2004)
- [3] S. Mukherjee, J.A. Stull, J. Yano, T.C. Stamatatos, K. Pringouri, T.A. Stich, K.A. Abboud, R.D. Britt, V.K. Yachandra, G. Christou, Proc. Natl. Acad. Sci. 109 (2012)
- [4] C. Zhang, C. Chen, H. Dong, J.-R. Shen, H. Dau, J. Zhao, Science 348 (2015) 690. [5] J.S. Kanady, E.Y. Tsui, M.W. Day, T. Agapie, Science 333 (2011) 733.
- [6] D. Gatteschi, L. Bogani, A. Cornia, M. Mannini, L. Sorace, R. Sessoli, Solid State Sci. 10 (2008) 1701.
- K. Sauer, J. Yano, V.K. Yachandra, Coord. Chem. Rev. 252 (2008) 318.
- R. Sessoli, D. Gatteschi, A. Caneschi, M.A. Novak, Nature 365 (1993) 141.
- [9] R. Sessoli, H.-L. Tsai, A.R. Schake, S. Wang, J.B. Vincent, K. Folting, D. Gatteschi, G. Christou, D.N. Hendrickson, J. Am. Chem. Soc. 115 (1993) 1804.
- [10] G. Christou, D. Gatteschi, D.N. Hendrickson, R. Sessoli, MRS Bull. 25 (2000) 66.
- [11] G. Christou, Polyhedron 24 (2005) 2065.
- [12] R. Bagai, G. Christou, Chem. Soc. Rev. 38 (2009) 1011.
- [13] (a) J.R. Friedman, M.P. Sarachik, J. Tejada, R. Ziolo, Phys. Rev. Lett. 76 (1996)
 - (b) L. Thomas, F. Lionti, R. Ballou, D. Gatteschi, R. Sessoli, B. Barbara, Nature 383 (1996) 145.
- [14] W. Wernsdorfer, S. Bhaduri, R. Tiron, D.N. Hendrickson, G. Christou, Phys. Rev. Lett. 89 (2002) 197201.
- [15] W. Wernsdorfer, R. Sessoli, Science 284 (1999) 133.
- [16] W. Wernsdorfer, M. Soler, G. Christou, D.N. Hendrickson, J. Appl. Phys. 91 (2002) 7164.
- [17] W. Wernsdorfer, N.E. Chakov, G. Christou, Phys. Rev. Lett. 95 (2005) 037203.
- [18] L. Lecren, W. Wernsdorfer, Y. Li, O. Roubeau, H. Miyasaka, R. Clerac, J. Am. Chem. Soc. 127 (2005) 11311.
- [19] S. Hill, R.S. Edwards, N. Aliaga-Alcalde, G. Christou, Science 302 (2003) 1015.
- [20] A. Wilson, S. Hill, R.S. Edwards, N. Aliaga-Alcalde, G. Christou, A.I.P. Conf, Proc. 850 (2006) 1141.
- [21] R. Tiron, W. Wernsdorfer, D. Foguet-Albiol, N. Aliaga-Alcalde, G. Christou, Phys. Rev. Lett. 91 (2003) 227203.
- [22] T. Lis, Acta Cryst. B 36 (1980) 2042.
- [23] G. Aromí, E.K. Brechin, Struct. Bond. 122 (2006) 1.
- [24] D. Gatteschi, R. Sessoli, J. Villain, Oxford Univ. Press (2006).
- [25] Z. Sun, D. Ruiz, E. Rumberger, C.D. Incarvito, K. Folting, A.L. Rheingold, G. Christou, D.N. Hendrickson, Inorg. Chem. 37 (1998) 4758.
- [26] Z. Sun, D. Ruiz, N.R. Dilley, M. Soler, J. Ribas, K. Folting, M.B. Maple, G. Christou, D.N. Hendrickson, Chem. Commun. (1999) 1973.
- [27] M. Soler, S.K. Chandra, D. Ruiz, E.R. Davidson, D.N. Hendrickson, G. Christou, Chem. Commun. (2000) 2417.
- [28] S. Bhaduri, M. Pink, G. Christou, Chem. Commun. (2002) 2352.
- [29] C. Boskovic, J.C. Huffman, G. Christou, Chem. Commun. (2002) 2502.

- (a) A. Vinslava, A.J. Tasiopoulos, W. Wernsdorfer, K.A. Abboud, G. Christou, Inorg, Chem. 55 (2016) 3419;
 (b) A.L. Tasiopoulos, A. Vinslava, W. Wernsdorfer, K.A. Abboud, G. Christou
 - (b) A.J. Tasiopoulos, A. Vinslava, W. Wernsdorfer, K.A. Abboud, G. Christou, Angew. Chem. Int. Ed. 43 (2004) 2117.
- [31] C.C. Stoumpos, T.C. Stamatatos, V. Psycharis, C.P. Raptopoulou, G. Christou, S.P. Perlepes, Polyhedron 27 (2008) 3703.
- [32] T.N. Nguyen, K.A. Abboud, G. Christou, Polyhedron 103 (2016) 150.
- [33] D.I. Alexandropoulos, A.M. Mowson, M. Pilkington, V. Bekiari, G. Christou, T.C. Stamatatos, Dalton Trans. 43 (2014) 1965.
- [34] T.C. Stamatatos, D. Foguet-albiol, C.C. Stoumpos, C.P. Raptopoulou, A. Terzis, W. Wernsdorfer, S.P. Perlepes, G. Christou, Polyhedron 26 (2007) 2165.
- [35] C. Lampropoulos, T.C. Stamatatos, M.J. Manos, A.J. Tasiopoulos, K.A. Abboud, G. Christou, Eur. J. Inorg. Chem. (2010) 2244.
- [36] C.C. Stoumpos, T.C. Stamatatos, H. Sartzi, O. Roubeau, A.J. Tasiopoulos, V. Nastopoulos, S.J. Teat, G. Christou, S.P. Perlepes, Dalton Trans. (2009) 1004.
- [37] T.C. Stamatatos, D. Foguet-Albiol, S.-C. Lee, C.C. Stoumpos, C.P. Raptopoulou, A. Terzis, W. Wernsdorfer, S.O. Hill, S.P. Perlepes, G. Christou, J. Am. Chem. Soc. 129 (2007) 9484.
- [38] T.N. Nguyen, W. Wernsdorfer, M. Shiddiq, K.A. Abboud, S. Hill, G. Christou, Chem. Sci. 7 (2016) 1156.
- [39] T.N. Nguyen, M. Shiddiq, T. Ghosh, K.A. Abboud, S. Hill, G. Christou, J. Am. Chem. Soc. 137 (2015) 7160.
- [40] A.M. Mowson, T.N. Nguyen, K.A. Abboud, G. Christou, Inorg. Chem. 52 (2013)
- [41] H.J. Eppley, H.-L. Tsai, N. de Vries, K. Folting, G. Christou, D.N. Hendrickson, J. Am. Chem. Soc. 117 (1995) 301.
- [42] C.J. Milios, T.C. Stamatatos, S.P. Perlepes, Polyhedron 25 (2006) 134.
- [43] G.A. Bain, J.F. Berry, J. Chem. Educ. 85 (2008) 532.
- [44] SHELXTL2014, Bruker-AXS, Madison, Wisconsin, USA, 2014.
- [45] P. Van Der Sluis, A.L. Spek, Acta Crystallogr. A 46 (1990) 194.
- [46] A.L. Spek, Acta Crystallogr. C 71 (2015) 9.
- [47] O.A. Adebayo, K.A. Abboud, G. Christou, Inorg. Chem. 56 (2017) 11352.
- [48] H.-S. Wang, Z.-C. Zhang, X.-J. Song, J.-W. Zhang, H.-B. Zhou, J. Wang, Y. Song, X.-Z. You, Dalton Trans. 40 (2011) 2703.
- [49] (a) W. Liu, H.H. Thorp, Inorg. Chem. 32 (1993) 4102; (b) I.D. Brown, D. Altermatt, Acta Cryst. B 41 (1985) 244.
- [50] A.W. Addison, T.N. Rao, J. Reedijk, J. van Rijn, G.C. Verschoor, J. Chem. Soc. Dalton Trans. (1984) 1349.
- [51] O. Roubeau, R. Clérac, Eur. J. Inorg. Chem. (2008) 4325.
- [52] (a) S. Wang, J.C. Huffman, K. Folting, W.E. Streib, E.B. Lobkovsky, G. Christou, Angew. Chem. Int. Ed. 30 (1991) 1672;
 - (b) R. Bagai, K.A. Abboud, G. Christou, Dalton Trans. (2006) 3306;
 - (c) M.W. Wemple, H.L. Tsai, W.E. Streib, D.N. Hendrickson, G. Christou, J. Chem. Soc. Chem. Commun. (1994) 1031;
 - (d) S. Wang, H.-L. Tsai, W.E. Streib, G. Christou, D.N. Hendrickson, J. Chem. Soc., Chem. Commun. (1992) 677.
- [53] O. Roubeau, L. Lecren, Y. Li, X.F. Le Goff, R. Clerac, Inorg. Chem. Commun. 8 (2005) 314.

- [54] X. Jiang, G. An, C. Liu, H. Kou, Eur. J. Inorg. Chem. (2015) 5314.
- [55] X.-T. Wang, H.-M. Dong, X.-G. Wang, E.-C. Yang, X.-J. Zhao, Z Anorg. Allg. Chem. 642 (2016) 1166.
- [56] S. Piligkos, G. Rajaraman, M. Soler, N. Kirchner, J. Van Slageren, R. Bircher, S. Parsons, H. Gudel, J. Kortus, W. Wernsdorfer, G. Christou, E.K. Brechin, J. Am. Chem. Soc. 127 (2005) 5572.
- [57] M. Murugesu, W. Wernsdorfer, G. Christou, E.K. Brechin, Polyhedron 26 (2007) 1845.
- [58] R. Inglis, F. White, S. Piligkos, W. Wernsdorfer, E.K. Brechin, G.S. Papaefstathiou, Chem. Commun. 47 (2011) 3090.
- [59] S. Wang, L. Kong, H. Yang, Z. He, Z. Jiang, D. Li, S. Zeng, M. Niu, Y. Song, J. Dou, Inorg. Chem. 50 (2011) 2705.
- [60] M. Holynska, N. Frank, C. Pichon, I.-R. Jeon, R. Clérac, S. Dehnen, Inorg. Chem. 52 (2013) 7317.
- [61] E.S. Koumousi, M.J. Manos, C. Lampropoulos, A.J. Tasiopoulos, W. Wernsdorfer, G. Christou, T.C. Stamatatos, Inorg. Chem. 49 (2010) 3077.
- [62] E.K. Brechin, G. Christou, M. Soler, M. Helliwell, S.J. Teat, Dalton Trans. (2003) 513.
- [63] C. Lampropoulos, T.C. Stamatatos, K.A. Abboud, G. Christou, Polyhedron 28 (2009) 1958.
- [64] N.E. Chakov, L.N. Zakharov, A.L. Rheingold, K.A. Abboud, G. Christou, Inorg. Chem. 44 (2005) 4555.
- [65] S. Huang, S. Jhan, C. Yang, H. Tsai, Polyhedron 66 (2013) 245.
- [66] F. Xiao, L. Jin, Inorg. Chem. Commun. 11 (2008) 717.
- [67] G. Aromí, A. Bell, S.J. Teat, A. Gavin, R.E.P. Winpenny, Chem. Commun. (2002) 1896.
- [68] D.I. Alexandropoulos, C. Papatriantafyllopoulou, C. Li, L. Cunha-Silva, M.J. Manos, A.J. Tasiopoulos, W. Wernsdorfer, G. Christou, T.C. Stamatatos, Eur. J. Inorg. Chem. (2013) 2286.
- [69] C.J. Milios, E. Kefalloniti, C.P. Raptopoulou, A. Terzis, R. Vicente, N. Lalioti, A. Escuer, S.P. Perlepes, Chem. Commun. (2003) 819.
- [70] J.S. Costa, L.A. Barrios, G.A. Craig, S.J. Teat, F. Luis, O. Roubeau, M. Evangelisti, A. Camon, G. Aromí, Chem. Commun. 48 (2012) 1413.
- [71] K. Su, F. Jiang, J. Qian, J. Pan, J. Pang, X. Wan, F. Hu, M. Hong, RSC Adv. 5 (2015) 33579
- [72] M. Manoli, A. Collins, S. Parsons, A. Candini, M. Evangelisti, E.K. Brechin, J. Am. Chem. Soc. 130 (2008) 11129.
- [73] Y. Okui, A. Catusanu, R. Kubota, B. Kure, T. Nakajima, T. Tanase, T. Kajiwara, M. Mikuriya, H. Miyasaka, M. Yamashita, Eur. J. Inorg. Chem. (2011) 4325.
- [74] L. Zhang, R. Clerac, P. Heijboer, W. Schmitt, Angew. Chem. Int. Ed. 51 (2012)
- [75] M.U. Anwar, Y. Lan, L.M.C. Beltran, R. Clérac, S. Pfirrmann, C.E. Anson, A.K. Powell, Inorg. Chem. 48 (2009) 5177.
- [76] M. Charalambous, E.E. Moushi, T.N. Nguyen, A.M. Mowson, G. Christou, A.J. Tasiopoulos, Eur. J. Inorg. Chem. (2018) 3905.